Optical *in situ* study of the reduction/oxidation processes in $YAlO_3$:Mn crystals

2009 J. Phys.: Condens. Matter 21 175411

(http://iopscience.iop.org/0953-8984/21/17/175411)

J. Phys.: Condens. Matter **21** (2009) 175411 (6pp) doi:10.1088/0953-8984/21/17/175411

Optical *in situ* study of the reduction/oxidation processes in $YAlO_3$:Mn crystals

Ya Zhydachevskii[1], O Buryy[1], D Sugak[2], S Ubizskii[1], A Börger[3], K-D Becker[3], A Suchocki[4,5] and M Berkowski[4]

[1] Lviv Polytechnic National University, 12 Bandera, Lviv 79646, Ukraine
[2] Institute of Materials, SRC 'Carat', 202 Stryjska, Lviv 79031, Ukraine
[3] Institute of Physical and Theoretical Chemistry, Technische Universität Braunschweig, D-38106 Braunschweig, Germany
[4] Institute of Physics, Polish Academy of Sciences, Aleja Lotników 32/46, Warsaw 02668, Poland
[5] Institute of Physics, University of Bydgoszcz, Weyssenhoffa 11, Bydgoszcz 85072, Poland

E-mail: crystal@polynet.lviv.ua (Ya Zhydachevskii)

Received 3 February 2009
Published 1 April 2009
Online at stacks.iop.org/JPhysCM/21/175411

Abstract
The paper presents experimental results on an *in situ* optical absorption study of the reduction/oxidation processes in $YAlO_3$:Mn crystals that are visible in the $Mn^{4+} \leftrightarrow Mn^{5+}$ recharging of manganese ions. The appearance of the Mn^{5+} absorption during annealing in an oxidizing atmosphere as well as its bleaching during annealing of the crystal in a reducing atmosphere have been studied in the temperature range from 800 to 1250 K. The oxidation and reduction kinetics are analyzed in the framework of the vacancies diffusion model and compared with the nominally pure and Nd-doped $YAlO_3$ crystals studied previously.

1. Introduction

It is well known that single crystals of yttrium orthoaluminate ($YAlO_3$), especially those obtained by the Czochralski method from slightly non-stoichiometric charges enriched with the rare-earth component ($Y_2O_3/Al_2O_3 \geqslant 1$), have a characteristic red–brown coloration [1–3]. This coloration leads to optical losses in the rare-earth doped $YAlO_3$ laser elements and, thus, worsens the lasing properties of the material [4, 5]. Annealing the crystals in a reducing atmosphere or in a vacuum can essentially reduce this coloration. On the other hand, annealing in air or oxygen intensifies the crystal coloration [3, 5].

Up to now the changes in optical absorption that take place in $YAlO_3$ crystals under the influence of reducing/oxidizing thermal treatments were usually studied at room temperature after a certain annealing procedure of the crystal. In our recent work, an *in situ* optical absorption study of reduction/oxidation processes in $YAlO_3$ and $YAlO_3$:Nd crystals has been performed [6]. In this work, the increase of the coloration intrinsic to the crystal has been studied *in situ* during annealing in an oxidizing atmosphere, as well as their bleaching during reduction of the crystal in the temperature range from 600 to 1000 K. The oxidation and reduction kinetics have been analyzed in the framework of different models, taking into account diffusion and quasi-chemical reactions of the absorbing centers. However, we were unable to get reliable values of the diffusion coefficient at various temperatures for the studied crystals.

In the present work, we study Mn-doped $YAlO_3$ crystals, because, in the case of this crystal, the reduction/oxidation processes can be observed thanks to the recharging of the manganese ions. In addition, it is also of interest to compare the results for $YAlO_3$:Mn crystals with the corresponding ones obtained previously for pure and Nd-doped $YAlO_3$ crystals.

Manganese ions in $YAlO_3$:Mn crystals may be present mainly in the form of Mn^{4+} ions in octahedral coordination (Al^{3+} positions) [7, 8]. In addition, Mn^{2+} or Mn^{3+} ions can be present in strongly distorted dodecahedral coordination (Y^{3+} positions) [7, 9]. In addition to Mn^{4+} ions, Mn^{5+} ions in octahedral coordination can also be observed as a result of photoionization of Mn^{4+} ions ($Mn^{4+} \rightarrow Mn^{5+} + e^-$), or as an intrinsic valence state of manganese, especially when divalent co-doping is used [10, 11].

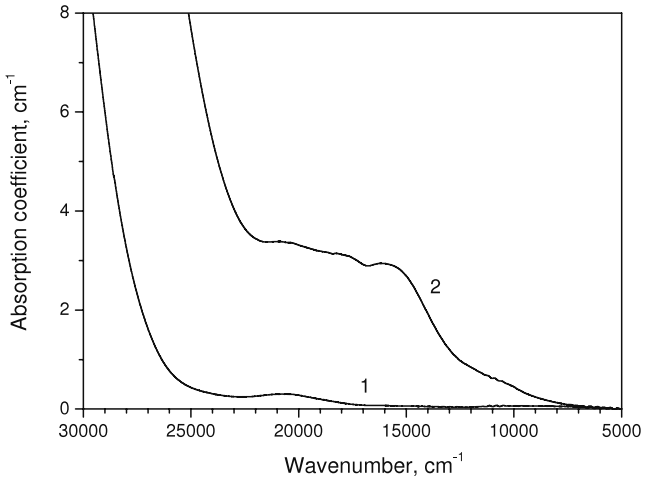

Figure 1. Optical absorption spectra of a (1) reduced and (2) oxidized $YAlO_3$:Mn crystal registered at room temperature.

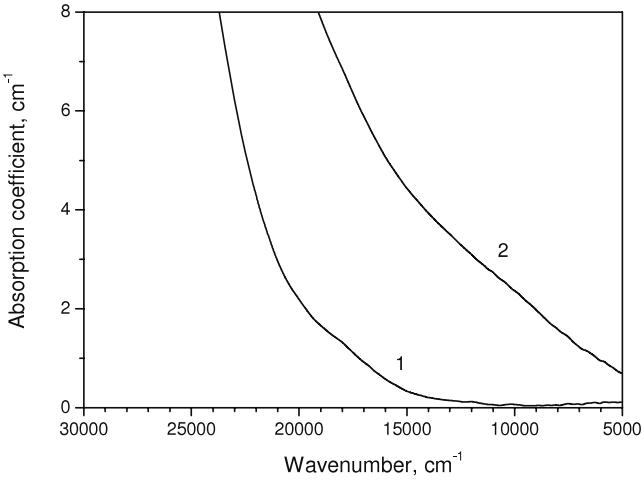

Figure 2. Optical absorption spectra of a (1) reduced and (2) oxidized $YAlO_3$:Mn crystal registered at $T = 1200$ K *in situ* in the reducing and oxidizing gas atmospheres, respectively.

As was shown previously in [12], high-temperature annealing of $YAlO_3$:Mn crystals in an oxidizing atmosphere results in the oxidation of the manganese ions ($Mn^{4+} \rightarrow Mn^{5+}$) present in the crystal. This becomes apparent in the strong absorption of Mn^{5+} ions in the visible region. The reducing annealing leads to the opposite recharging of manganese ions in such a way that the Mn^{5+} ions are completely removed. A charge compensation of the $Mn^{4+} \leftrightarrow Mn^{5+}$ recharging is obviously provided by an uptake (loss) of oxygen into (from) the crystal.

The present work is devoted to the *in situ* study of the $Mn^{4+} \leftrightarrow Mn^{5+}$ recharging processes in $YAlO_3$:Mn crystals under the reducing/oxidizing high-temperature treatments, in order to get better insight into the diffusion processes in the material.

2. Experimental details

The studied $YAlO_3$:Mn single crystals were grown by the Czochralski method in a pure nitrogen atmosphere by the technology described in [12]. The manganese concentration in the crystal corresponds to 0.2 at.% in the melt with respect to the aluminum content. Samples for investigation were prepared as flat-parallel plates of 1.5 mm thickness with polished surfaces.

The optical *in situ* experiments have been performed using a specially designed high-temperature furnace placed in a Perkin-Elmer Lambda 900 spectrophotometer, see [6] for details. The furnace allowed the heating of samples from room temperature up to 1250 K in controlled gas atmospheres. The gas supply system with controlled flow provides a well-defined atmosphere in the furnace. The main feature of the set-up is the possibility of rapid (∼1 min) replacement of gas atmospheres in the furnace, and the registration of the subsequent reduction/oxidation kinetics at a certain wavelength. The high-temperature absorption spectra were corrected for the radiation emitted by the sample and furnace at this temperature. Pure oxygen, O_2(g), was used as the oxidizing atmosphere and a mixture of gases 95%Ar + 5%H_2 was used as the reducing one.

3. Results and discussion

3.1. Experimental observation of the reduction/oxidation processes in $YAlO_3$:Mn

The optical absorption spectra of the studied $YAlO_3$:Mn crystal registered at room temperature are shown in figure 1. Curve 1 in the figure was measured after annealing of the sample in reducing atmosphere (30 min at $T = 1250$ K) and cooling down to room temperature. In the same way, curve 2 was measured after annealing in oxidizing atmosphere. As it will be shown below, the temperature and duration of annealing used here is enough to obtain a state with maximal (minimal) intensity of the Mn^{5+} ions absorption named hereafter as the oxidized (reduced) state of crystal.

The Mn^{4+} ions are responsible for the absorption band centered at about 21 000 cm^{-1} (transition $^4A_2 \rightarrow {}^4T_2$ [8]). The Mn^{5+} ions present in the oxidized crystal are responsible for the absorption bands near 12 000, 15 000, 18 000 and ∼26 000 cm^{-1} (transitions $^3T_1(^3F) \rightarrow {}^3T_2(^3F)$, $^3T_1(^3F) \rightarrow {}^3T_1(^3P)$, and $^3T_1(^3F) \rightarrow {}^3A_2(^3F)$ [10]). The intense absorption in the UV region is caused by O–Mn charge-transfer bands [8].

Figure 2 shows the absorption spectra of a reduced and oxidized $YAlO_3$:Mn crystal registered *in situ* at $T = 1200$ K in reducing and oxidizing atmospheres after saturation of absorption changes caused by the annealing. The spectrum of the oxidized crystal demonstrates an evident broadening and a shift of the Mn^{5+} absorption bands to the low-energy range.

The wavenumber of 15 000 cm^{-1} was chosen for registration of absorption changes caused by the oxidizing (reducing) annealing. The process of crystal oxidation, i.e. the process of the formation of Mn^{5+} ions, during heating of the reduced crystal in the oxidizing atmosphere is shown in figure 3. As is seen from the figure, at first some bleaching

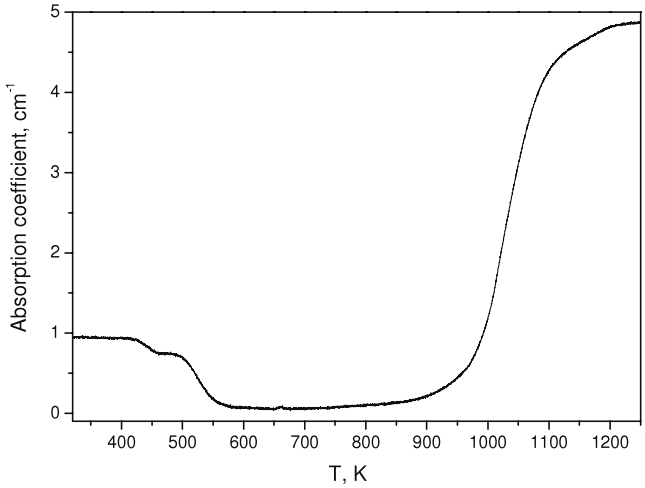

Figure 3. The optical absorption of a $YAlO_3$:Mn crystal registered at 15 000 cm^{-1} as a function of temperature during heating of the reduced crystal in an oxidizing atmosphere at a constant rate of 0.155 K s^{-1}.

of the crystal is observed in the 400–600 K temperature range. This bleaching agrees well with the temperature-induced decay of Mn^{5+} ions in the crystal previously exposed to visible light [12]. It should be noted, that in the spectrophotometer used, a monochromator was placed in the optical pathway after the sample, therefore the full-spectrum white beam illuminated the sample during the measurment time. In this way, some photocoloration of the crystal, caused by the $Mn^{4+} \rightarrow Mn^{5+}$ photoionization, can take place. Therefore, we interpret the observed bleaching of the crystal in the 400–600 K temperature range as the removal of the photoinduced Mn^{5+} ions. After that, the crystal remains colorless during heating up to 800 K. Above 850 K, an essential increase of the Mn^{5+} absorption occurs, which, in fact, is caused by the crystal oxidation.

The oxidation and reduction kinetics measured just after switching the gas atmosphere from a reducing to an oxidizing one, and conversely, at various temperatures are presented in figure 4. All the measured kinetics represent monotonic exponential-like curves of the absorption increase (decrease) during oxidation (reduction). It is should noted, however, that the reduction process occurs somewhat faster than the oxidation process at the same temperature.

The absorption changes shown in figures 1 and 2 are reversible. This means that the repeated replacement of the gas atmosphere from a reducing one to an oxidizing one and vice versa gives the same reduced and oxidized states of the crystal, as long as the annealing temperature and duration are sufficient to reach saturation of the absorption changes. We have not observed any changes of the sample surfaces after this kind of treatment at the temperatures used.

It should be noted that the coloration of the $YAlO_3$ crystal in the visible region, caused by intrinsic color centers, starts to increase during the oxidizing annealing already above 700 K [6]. When we assume that the same diffusion processes take place in $YAlO_3$ [6] and in the $YAlO_3$:Mn crystals studied here, we can expect redox processes to start at the same or similar temperatures. However, the reduction (oxidation)

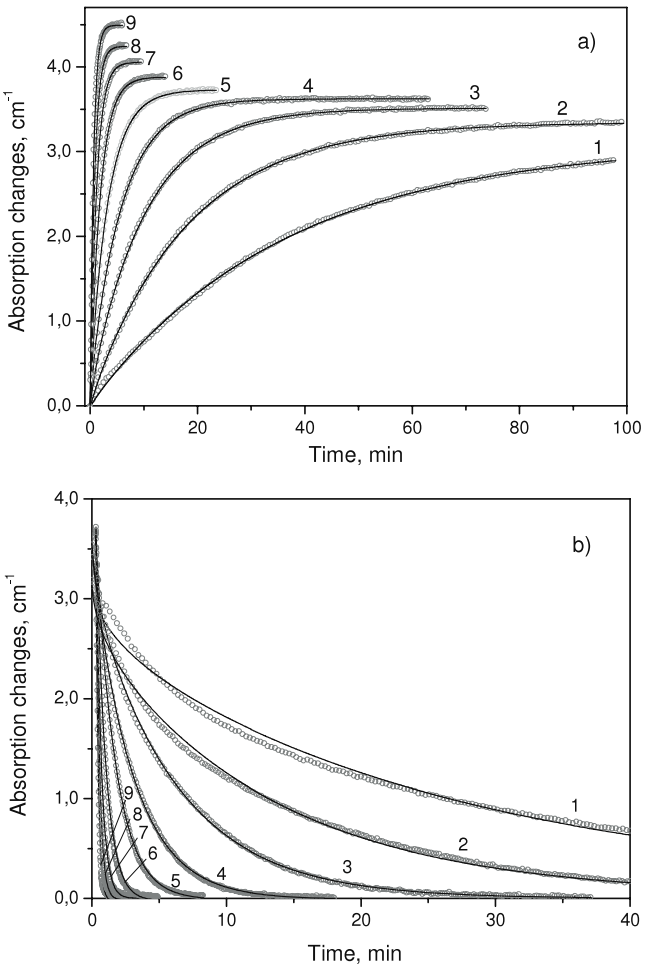

Figure 4. The oxidation (a) and reduction (b) kinetics registered at 15 000 cm^{-1} at various temperatures: 1—890 K, 2—930 K, 3—970 K, 4—1010 K, 5—1050 K, 6—1100 K, 7—1150 K, 8—1200 K, 9—1250 K, and their theoretical approximation by the diffusion model (see the text for details).

processes in $YAlO_3$:Mn crystals starts with noticeable speed at temperatures about 150 K higher than in pure or Nd-doped $YAlO_3$ crystals. Possible reasons for this discrepancy will be discussed below.

3.2. Diffusion model of the reduction/oxidation processes in $YAlO_3$:Mn

The observed reduction/oxidation kinetics has been analyzed in the framework of the diffusion model. The main assumptions and properties of this model are the following:

(1) During the oxidizing/reducing annealing of $YAlO_3$:Mn oxygen incorporation/excorporation processes take place. Depending on the charge state of the vacancies the following possible processes may occur at the crystal surface:

$$0.5O_2(g) + V_O^{\times} \leftrightarrow O_O^x, \qquad (1a)$$

$$0.5O_2(g) + V_O^{\bullet\bullet} \leftrightarrow O_O^x + 2h^{\bullet}, \qquad (1b)$$

$$0.5O_2(g) + V_O^{\bullet} \leftrightarrow O_O^x + h^{\bullet}, \qquad (1c)$$

$$1.5O_2(g) \leftrightarrow 3O_O^x + 2V_C''' + 6h^\bullet. \quad (1d)$$

Here V_O and V_C indicate the oxygen and cation vacancies, respectively.

(2) Simultaneous out-diffusion of charged anion vacancies and in-diffusion of holes and, possibly, cation vacancies during oxidation leads to recharging of manganese ions

$$h^\bullet + Mn^{4+} \rightarrow Mn^{5+}. \quad (2)$$

In the case of the surface process with neutral vacancy participation (1*a*), both manganese ions and vacancies are involved in the recharging process:

$$Mn^{4+} + V_O^\bullet \rightarrow Mn^{5+} + V_O^\times, \quad (3)$$

with subsequent out-diffusion of the neutral vacancy. During reduction processes (2)–(3) are reversed.

(3) The change of the Mn^{5+} concentration N_{Mn} is proportional to the change in vacancy concentration by:

$$\frac{\partial N_{Mn}}{\partial t} = -\kappa \frac{\partial N}{\partial t}, \quad (4)$$

where κ is a coefficient of proportionality.

(4) The diffusion of vacancies is described by the one-dimensional diffusion equation (second Fick law) [13]:

$$\frac{\partial N}{\partial t} = D\frac{\partial^2 N}{\partial^2 x}. \quad (5)$$

The initial condition for equation (5) is $N(t = 0, x) = N_0$, where N_0 is the concentration of vacancies in the crystal before annealing.

The boundary conditions for equation (5) correspond to the fact that the diffusant flow is continuous at the crystal surface. In accordance with the terminology of [13], they are third order boundary conditions

$$\begin{aligned} D\frac{\partial N}{\partial x}\bigg|_{x=0} &= R(N|_{x=0} - N_\infty), \\ -D\frac{\partial N}{\partial x}\bigg|_{x=d} &= R\,(N|_{x=d} - N_\infty), \end{aligned} \quad (6)$$

where d is the crystal thickness, N_∞ is the stationary concentration of vacancies achieved during annealing, in the oxidized crystal, obviously, $N_0 \approx 0$, R is the mass-transfer coefficient. If ratio Rd/D is about 10^2 or higher, the condition (6) transforms to the first order one $N|_{x=0,d} = N_\infty$.

Taking into account the solutions of (5) [13], the spatial and time dependency of Mn^{5+} concentration obtained from (4) is

$$N_{Mn}(x,t) = N_{Mn0} + \kappa\,(N_\infty - N_0)\sum_{k=0}^{\infty}\frac{4h}{d\left(h^2+\lambda_k^2\right)+2h} \times \left(\cos\lambda_k x + \frac{h}{\lambda_k}\sin\lambda_k x\right)\exp\left(-D\lambda_k^2 t\right), \quad (7)$$

where N_{Mn0} is the initial concentration of Mn^{5+} in the crystal, $h = R/D$ and λ_k are the characteristic values of the Sturm–Liouville problem determined by

$$tg\,(\lambda_k d) = \frac{2h\lambda_k}{\lambda_k^2 + h^2}. \quad (8)$$

The changes of the absorption coefficient $\Delta\alpha(t)$ due to changes in the concentration of Mn^{5+} ions is thus determined as

$$\Delta\alpha(t) = \frac{\sigma}{d}\int_0^d N_{Mn}(t,x)\,dx - \sigma N_{Mn0}, \quad (9)$$

where σ is the absorption cross-section.

Substituting (7) into (9) one can obtain:

$$\Delta\alpha(t) = \frac{\sigma}{d}\kappa\,(N_\infty - N_0) \times \sum_{k=0}^{\infty}\frac{8h^2}{d(h^2+\lambda_k^2)+2h}\frac{1}{\lambda_k^2}\exp(-D\lambda_k^2 t). \quad (10)$$

The expression (10) was used for the approximations of the experimental kinetics with fitting parameters D, $h_d = hd$ and $\Delta\alpha_0 = \frac{\sigma}{d}\kappa(N_\infty - N_0)$. The fitting accuracy is estimated by the χ^2 criterion [14]:

$$\chi^2 = \frac{1}{n - n_{var}}\sum_{i=1}^{n}\left(\Delta\alpha\,(t_i) - \Delta\alpha_i^{exp}\right)^2, \quad (11)$$

where n is the number of experimental points for which the fitting is carried out, n_{var} is the number of the fitting parameters, $\Delta\alpha(t)$ is the fitting function, and $\Delta\alpha_i^{exp}$ is the experimental value of the absorption coefficient change at time t_i.

The standard error of the determination of the fitting parameters is estimated as

$$\sigma_j = \sqrt{C_{jj}\chi^2}, \quad (12)$$

where j is the number of the fitting parameter, $j = 1, \ldots, 3$, C_{jj} is the diagonal element of the variance–covariance matrix determined as $C = (J_T J)^{-1}$, J—Jacobian, i.e. the matrix with the elements $\partial(\Delta\alpha(t_i))/\partial x_j$, and x_j is the fitting parameter [14].

The results of fitting are shown in figure 4 as solid lines. The values of the χ^2 criterion and diffusion coefficients obtained, as well as their standard errors σ_j are presented in table 1. It should be mentioned, that for some experimental kinetics, the obtained values of standard errors for D and h_d are higher than the absolute values of the corresponding fitting parameters. Thus, the parameters cannot be determined correctly and such cases are marked by a dash in table 1.

As it is seen from figure 4 and table 1, fitting is noticeably better for the case of oxidation than for reduction. This fitting allows all relevant parameters for most of the oxidation kinetics to be correctly determined.

Figure 5 shows the temperature dependencies of the diffusion coefficients obtained for vacancies D in Arrhenius coordinates. The value of the activation energy for diffusion obtained from the approximation of these dependencies (for the reduction and oxidation simultaneously) is equal to 1.34 ± 0.17 eV.

The fact that this simple diffusion model provides quite a good fit to the experimental kinetics observed in $YAlO_3$:Mn crystals enables us to consider the $Mn^{4+} \leftrightarrow Mn^{5+}$ recharging process to be determined only by the vacancies diffusion during the oxidation and reduction processes. Note that the predominant type of vacancy (oxygen or cation) cannot be determined from our experiments.

Table 1. Diffusion coefficients and approximation accuracies.

	Oxidation		Reduction	
T (K)	D (cm^2 s^{-1})	χ^2	D (cm^2 s^{-1})	χ^2
890	$(3.77 \pm 0.05) \times 10^{-6}$	9.7×10^{-7}	$(1.410 \pm 0.006) \times 10^{-6}$	9.04×10^{-6}
930	$(5.48 \pm 0.04) \times 10^{-6}$	6.8×10^{-7}	$(2.90 \pm 0.01) \times 10^{-6}$	3.97×10^{-6}
970	$(6.57 \pm 0.03) \times 10^{-6}$	5.9×10^{-7}	$(7.60 \pm 0.04) \times 10^{-6}$	1.74×10^{-6}
1010	$(9.98 \pm 0.03) \times 10^{-6}$	3.6×10^{-7}	$(3.08 \pm 0.01) \times 10^{-5}$	2.66×10^{-6}
1050	$(1.735 \pm 0.007) \times 10^{-5}$	3.5×10^{-7}	—	1.23×10^{-6}
1100	$(4.41 \pm 0.08) \times 10^{-5}$	1.02×10^{-6}	—	1.014×10^{-5}
1150	$(1.92 \pm 0.3) \times 10^{-4}$	1.47×10^{-6}	—	8.72×10^{-6}
1200	—	2.95×10^{-6}	—	1.830×10^{-5}
1250	—	1.247×10^{-5}	—	2.485×10^{-5}

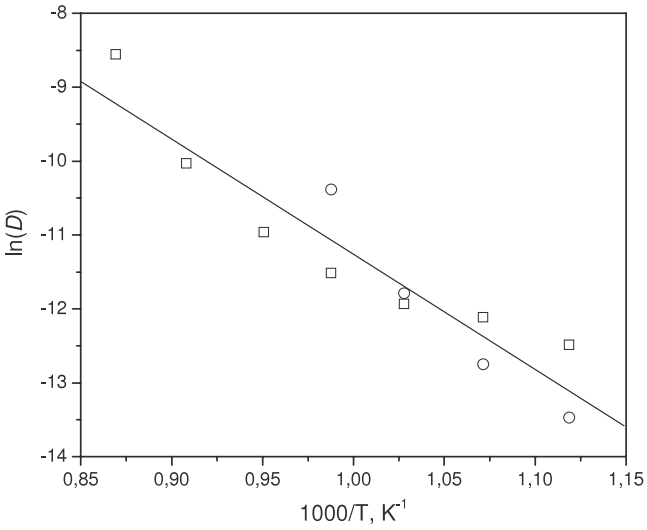

Figure 5. Arrhenius plot for the diffusion coefficients for oxidation (squares) and reduction (circles) processes, and their linear approximation. Here error bars for the values of the diffusion coefficients do not exceed sizes of the symbols used.

In the case of the intrinsic color centers in pure or Nd-doped $YAlO_3$ crystals, the situation is much more complicated. As was shown in [6], an approximation in the framework of the same diffusion model does not provide an adequate fit of the experimental data for these crystals. Let us recall that an acceptable description of the experimental data for these crystals was obtained from two different models. The first of them assumes two diffusion mechanisms, one fast and one slow, with the participation of two species of defects, possibly oxygen and cation vacancies. The second model takes into consideration not only diffusion but also the quasi-chemical reactions of defects [6].

Notwithstanding these problems, we established the fact that the reduction (oxidation) process in nominally pure or Nd-doped $YAlO_3$ crystals starts at lower temperatures and occurs noticeably faster than in the $YAlO_3$:Mn crystals studied here. When the assumption is made of the existence of two diffusion mechanisms with the participation of oxygen or cation vacancies, one can explain the aforementioned discrepancy between $YAlO_3$ and $YAlO_3$:Mn crystals by assuming that in the latter, only one type of vacancy is contributing to the transport. However, this discrepancy between nominally pure crystals and Mn-doped $YAlO_3$ is not obvious to us. Possibly it is due to the fact that the absorbing centers in each of these crystals require different charge compensation.

4. Conclusions

The studies performed on the reduction/oxidation processes in $YAlO_3$:Mn crystals revealed the following features.

The recharging of manganese ions ($Mn^{4+} \leftrightarrow Mn^{5+}$) as a result of the reducing/oxidizing thermal treatment starts with noticeable speed at temperatures above 850 K. The reduction process occurs somewhat faster than the oxidation one at the same temperature.

It is considered that the $Mn^{4+} \leftrightarrow Mn^{5+}$ recharging process during oxidation or reduction is determined by the incorporation/excorporation of oxygen and the diffusion of oxygen or cation vacancies. Also, the reduction (oxidation) process in $YAlO_3$:Mn crystals begins at higher temperatures and occurs noticeably more slowly than in the nominally pure or Nd-doped $YAlO_3$ crystals previously studied by us.

Unlike the $YAlO_3$ crystals studied previously, the approximation of the experimental reduction and oxidation kinetics of $YAlO_3$:Mn by a simple diffusion model, which accounts for the vacancies diffusion only, provides quite a good fit to the experimental data.

Diffusion coefficients obtained here for the majority of the experimental kinetics (oxidation and reduction) in the temperature range from 890 to 1250 K were found to possess activation energy of 1.34 ± 0.17 eV. At the same time, the approximation by the diffusion model for the oxidation process is rather better than that for the reduction process.

Acknowledgments

The work was supported by the Ukrainian Ministry of Education and Science (projects DB/Tern and M/53-2008), by the German Ministry of Education and Research (WTZ Project UKR 06/003) and by a grant from the Polish Ministry of Science and Education for the years 2006–2009.

References

[1] Li G, Shi Z, Guo X, Wu J, Chen Y and Chen J 1990 *J. Cryst. Growth* **106** 524
[2] Li G, Guo X, Lu J, Shi Z, Wu J, Chen Y and Chen J 1992 *J. Cryst. Growth* **118** 371

[3] Savytskii D I, Vasylechko L O, Matkovskii A O, Solskii I M, Suchocki A, Sugak D Yu and Wallrafen F 2000 *J. Cryst. Growth* **209** 874
[4] Kvapil J, Kvapil J, Perner B, Manek B, Blazek K and Hendrich Z 1985 *Cryst. Res. Technol.* **20** 473
[5] Sugak D, Matkovskii A, Savitskii D, Durygin A, Suchocki A, Zhydachevskii Y, Solskii I, Stefaniuk I and Walraffen F 2001 *Phys. Status Solidi* a **184** 239
[6] Sugak D, Zhydachevskii Ya, Buryy O, Ubizskii S, Börger A, Schrader M and Becker K D 2008 *Acta Mater.* **56** 6310
[7] Rakhimov R R, Wilkerson A L, Loutts G B, Noginov M A, Noginova N, Lindsay W and Ries H R 1998 *Solid State Commun.* **108** 549
[8] Noginov M A and Loutts G B 1999 *J. Opt. Soc. Am.* B **16** 3
[9] Noginov M A, Loutts G B and Warren M 1999 *J. Opt. Soc. Am.* B **16** 475
[10] Noginov M A, Loutts G B, Noginova N, Hurling S and Kuck S 2000 *Phys. Rev.* B **61** 1884
[11] Noginov M A, Loutts G B, Ross K, Grandy T, Noginova N, Lucas B D and Mapp T 2001 *J. Opt. Soc. Am.* B **18** 931
[12] Zhydachevskii Ya, Suchocki A, Sugak D, Luchechko A, Berkowski M, Warchol S and Jakiela R 2006 *J. Phys.: Condens. Matter* **18** 5389
[13] Crank J 1955 *The Mathematics of Diffusion* (Oxford: Oxford University Press)
[14] Press W H, Flannery B P, Teukolsky S A and Vetterling W T 1989 *Numerical Recipes in Pascal. The Art of Scientific Computing* (Cambridge: Cambridge University Press)